PHOTONIC SENSORS / Vol. 9, No. 1, 2019: 60–68

Resonant Light Scattering Toward Optical Fiber Humidity Sensors

Mahboubeh DEHGHANI SANIJ[1*], Abolfazl BAHRAMPOUR[2], and Ali Reza BAHRAMPOUR[2]

[1]*Faculty of Physics, Shahid Bahonar University of Kerman, Kerman 7616914111, Iran*

[2]*Department of Physics, Sharif University of Technology, Tehran 1458889694, Iran*

[*]Corresponding author: Mahboubeh DEHGHANI SANIJ E-mail: mahdehsanij@gmail.com

Abstract: The deposition of tetrakis (4-sulonatophenyl) porphyrin (TPPS) thin film on optical fibers presents many possibilities for sensing applications. The J-form aggregation with a narrow and sharp spectral feature at about 490 nm and its sensitivity to humidity have been discussed; a fast change of wavelength occurs according with variation in the humidity level. The reproducibility and high sensitivity of TPPS-coated fibers, along with the capabilities of optical fibers, suggest the device as a good candidate for humidity sensing in harsh environments.

Keywords: Humidity; chemical; porphyrin-based; chemical optical fiber sensor

Citation: Mahboubeh DEHGHANI SANIJ, Abolfazl BAHRAMPOUR, and Ali Reza BAHRAMPOUR, "Resonant Light Scattering Toward Optical Fiber Humidity Sensors," *Photonic Sensors*, 2019, 9(1): 60–68.

1. Introduction

The measurement and control of humidity levels in different environments are important in many fields, including agriculture, environmental science, and the oil and gas industries. To ensure safety, increase the lifetime of materials, and improve irrigation in agricultural fields, different application-specific techniques for humidity control with different sensitivities are used.

Optical fiber sensors are small in size, insensitive to electromagnetic interference, and capable of multi-parameter sensing, and are thus good candidates for environmental monitoring [1]. Chemical optical fiber sensors, among the most intriguing applications of optical fibers, have attracted significant research attention. Chemical sensors cannot be efficient and valuable without the right selectivity. Fiber optics are potentially good candidates for selective and sensitive sensors by combining the optical transducer with active materials selected and arranged to detect specific chemicals [2, 3].

Several approaches have been reported to detect and measure relative humidity (RH) using optical fiber sensors. These include direct spectroscopy of the absorbance band of water [4–7] and unclad fibers detecting evanescence modes [8–13]. Several researchers have reported some fiber sensor arrangements with and without integrating materials on long-period fiber Bragg gratings [14–17]. Among different sensing materials available in the optical technology, porphyrin molecules and derivatives thereof have recently shown good properties for the integration with the optical fiber technology in developing novel sensing probes [18–24]. The

Received: 7 April 2018 / Revised: 4 August 2018

DOI: 10.1007/s13320-018-0519-4
Article type: Regular

deposition of layers of such compounds has been achieved through several techniques including physical vapor deposition (PVD), chemical vapor deposition (CVD) [25], layer-by-layer electrostatic deposition [26], and the self-assembly of monolayers [27]. A non-conventional approach via the ultraviolet(UV)-induced deposition of tetrakis (4-sulonatophenyl) porphyrin (TPPS) molecules is also demonstrated, with the growth of discrete crystals generating uniform thin films of TPPS molecules on different substrates [28, 29].

Recent investigations into the deposition of TPPS molecules on optical fibers using UV lasers have shown new possibilities for optical sensing [30–33]. The TPPS molecule can switch between different aggregate forms in response to the presence of acidic or basic vapors, namely the J- and H-type aggregates, which present distinctive spectral features [34].

In the present work, the spectral features of the J-aggregate are investigated as a function of the local RH. This extends the functionality of thin TPPS layers integrated with optical fibers. The integration of such a simple and inexpensive humidity sensor with an optical fiber transmission line permits employment in internet-of-things (IoT) applications, in harsh environments and in irrigation as a component of intelligent agricultural engineering. In intelligent farms, many humidity sensors are required to transmit humidity data through the internet and thereby control farm irrigation.

2. Theoretical background

In the mid-1930s, Scheibe [35, 36] and Jelley [37] independently discovered the appearance of a narrow absorption band with an increase in the concentration of pseudoisocyanine (PIC) dye in water. The narrow-band absorption is redshifted relative to the monomer band. This effect is ascribed to the optical excitation of formed aggregates, which are clusters of molecules of intermediate size between crystals and isolated molecules. Aggregates are formed by the dipole-dipole interaction of monomers [38, 39]. Based on the spectral shift of the aggregate absorption peak relative to the maximum absorption of the monomer, the aggregates are classified as J- and H-types, corresponding to red and blue spectral shifts, respectively. J- and H-aggregates are further distinguished by the angle θ between the molecular transition dipole moment and the long aggregate axis. In some substances, such as PIC and TPPS, both J- and H-aggregates are found. The J- and H-aggregates of TPPS form in basic and acidic solvents, respectively [30–33], and show the angles $\theta > 54.7^\circ$ and $\theta < 54.7^\circ$. Dipole-dipole interactions between two or more monomers in an aggregate unit cell [40, 41] cause the coupling of excitons and vibrational levels of the monomers. The coupling coefficients depend on the intermolecular distance, the number of interacting molecules, and the angle between the transition dipole moment and the aggregate axis. In the absence of exciton coupling coefficients, the exciton states are degenerate, and only one maximum is observed in the absorption spectrum. The coupling of excitons causes energy level splitting, which introduces several peaks to the absorption spectrum. Both theoretical and experimental investigations show that the J-band appears with exciton coupling and without vibrational-mode coupling of monomers. In the J-aggregates, the energy transfer by excitons along the monomers in the cooperative excitonic state is sufficiently rapid to suppress vibrational relaxation before energy is transferred to the next monomer; therefore, the effects of vibrational level broadening are negligible. However, the H-aggregate absorption spectrum cannot show the absence of vibrational mode coupling. The J-aggregate shift is determined by the coupling strength, which is simply given as [41]

$$C = \sum_{n,m} V_{nm} \tag{1}$$

where V_{nm} is the matrix element of the total dipole-dipole interaction operator V, and n denotes the position of the nth monomer in a periodic lattice with one monomer per unit cell. C is affected by environmental disturbances.

Suitable methods can be employed to deposit J- or H-aggregate in the solid form. Experimental investigations have shown that the coupling strength C in J-aggregated TPPS varies with the environmental RH, with the absorption peak variation demonstrating this sensitivity. The Kramer-Korning relation also predicts that increased RH affects the refractive index of J-aggregated TPPS; thus, the reflectance coefficient also changes with RH. Variations of both the absorption frequency peak and reflectance versus RH can be employed in the design of new humidity sensors. In the following sections, such a humidity sensor design is proposed, and its capability is verified experimentally.

3. Methods

3.1 UV-induced TPPS deposition on the fiber tip

Various controllable coating techniques for porphyrin molecules have been reported for use on optical fiber tips [42, 43]. In this section, we describe the development of the UV-induced deposition of TPPS molecules on optical fiber (200 μm core, Ocean Optics P200-2-UV-VIS) end [32, 33]. Briefly, the fiber is cleaved by a standard cleaver (Xinyufei Fiber Optic Cleaver D6) and has been kept clean in dichloromethane (CH_2Cl_2) TPPS molecular film deposition obtained by dipping the cleaved tip of the multimode fiber in a tetrabutylammonium solution in CH_2Cl_2 with a concentration of 5 mol/L – 10 mol/L, followed by irradiation with a He-Cd 325 nm 9.5 mW UV laser (Melles Griot) coupled to the fiber optics. Figure 1 depicts the deposition setup schematically. For IoT applications, the same method can be employed with a single-mode fiber to match the humidity sensor and transmission line fiber. For simplicity in this experimental investigation, a multi-mode fiber is employed.

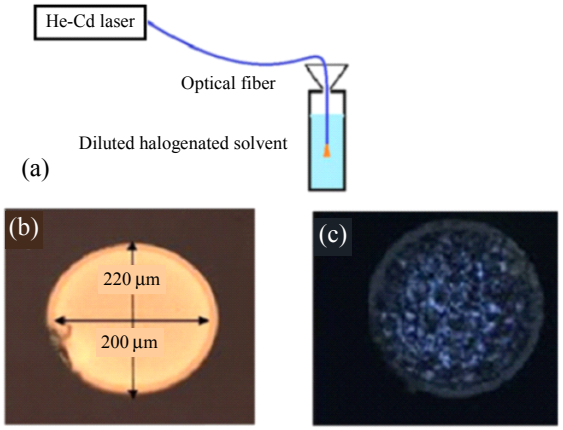

Fig. 1 Setup and microscopic observation of the fiber distal end: (a) schematic of UV-induced deposition on the optical fiber terminal end, (b) optical fiber transversal cross-section with a 200 μm core and 220 μm clad diameters, and (c) representation of the optical fiber terminal end after TPPS thin-film deposition.

3.2 Sample preparation and characterization

We employ a nonstandard multi-mode ultraviolet/visible optical fiber with a 200 μm core prepared by a fiber cleaver, as described in Section 3, for TPPS deposition. The core and cladding diameters of the UV/VIS fiber are 200 μm and 220 μm, respectively. The optical fiber guides UV radiation to the fiber tip, thus stimulating the local precipitation of molecules for deposition on the fiber core. The multi-mode fiber is situated in a diluted solution (5 μmol/L − 10 μmol/L) of the tetrabutylammonium salt of TPPS in CH_2Cl_2 during UV laser irradiation. A 9.5 mW He-Cd laser is used as the UV radiation source.

Investigating several irradiation durations shows that 60 min UV irradiation provides the best morphological results. The microscopic observation of the deposited distal end is shown in Fig. 1(c). The self-aligned thin film on the fiber core is detectable in Figs. 1(b) and 1(c), with the separation line matching the core-cladding border because of UV photochemical effects during deposition, as previously reported [32, 33].

To characterize the TPPS thin film deposited on the fiber tip, a reflectance scattering spectroscopy is employed, comparing the scattering spectra obtained before and after TPPS deposition. Figure 2 shows a schematic of the experimental setup for the reflectance scattering spectroscopy. A visible light source in the range of 400 nm – 800 nm with a nearly Gaussian distribution is used. The spectrum of the light source is saved for data normalization.

As shown in Fig. 2, the broadband light source and Avantes spectrometer (AvaSpec mod 2048) are coupled using a 50% 2×1 coupler (220 μm Ocean Optics UV-VIS) to the deposited fiber. The fiber end is illuminated by a broadband light source, and 50% of the reflected light source is detected by an optical spectrometer.

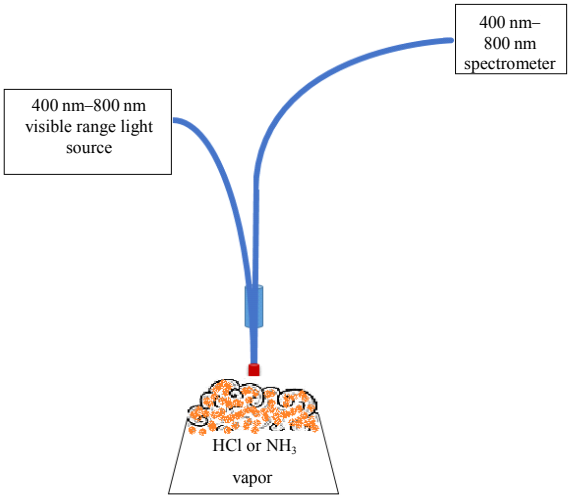

Fig. 2 Spectroscopy setup for reflectance analysis of acid and base exposure.

The reflectance spectra of the uncoated and TPPS-coated fibers are shown in Fig. 3. Spectral analysis of the film shows differences in optical amplitude, but the presence of Soret bands at 420 nm and 490 nm [30], and characteristic of the J-aggregate, are not observable; no special feature is observed in the blue band.

As shown in Fig. 3, J-aggregate bands [28] are not observed in the reflectance spectrum. The absorption spectrum of TPPS J-aggregates is depicted in Fig. 4 [40].

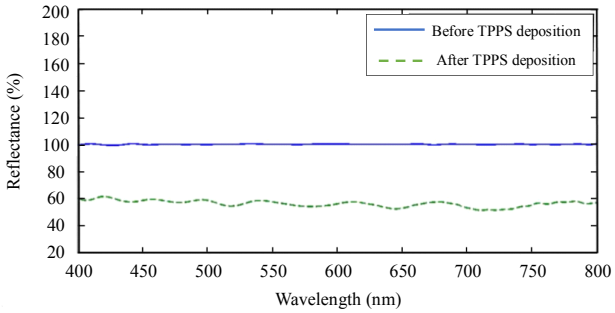

Fig. 3 Reflectance spectra of TPPS deposited on the fiber end.

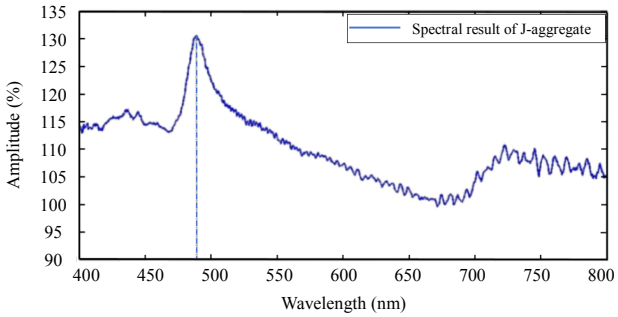

Fig. 4 J-aggregate spectral results.

Post-deposition treatment is performed to obtain the J- and H-aggregate bands in the reflectance spectrum [32]. The reflectance spectrum is observed at each step of treatment. In this preparation, all physical and chemical parameters are fully controlled. As detailed in Section 5, the temperature and humidity during the treatment are fixed at 22 ℃ and 80%, respectively. The post-deposition treatment is given by the following steps:

(1) The thin film is exposed directly to the ammonia vapor for 2 min to form an H-aggregate film;

(2) The deposited fiber is placed in air for 5 minutes;

(3) The film is exposed to the hydrochloric acid for protonation. The remaining basic and acidic species react to produce salt and water on the thin film. Steps (1) to (3) are repeated until the resonance light scattering peak at about 490 nm, indicating J-aggregate formation, reaches its maximum intensity in agreement with the results reported

elsewhere. The strength of the Soret band is low relative to that of the 490 nm band [30]. The J- and H-aggregates and corresponding energy levels [31] are presented in Fig. 5.

This treatment is previously reported for an acid- and base-detecting sensor [32]. We examine the ability of the prepared J-aggregate TPPS-coated optical fiber sample to measure humidity [32, 33, 44].

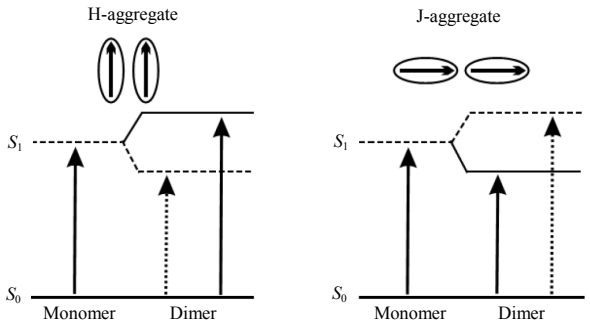

Fig. 5 H-aggregate, J-aggregate, and corresponding energy levels.

3.3 Sensing characterization of humidity variations

The sensing capability of the TPPS-coated fiber tip to RH is explored by monitoring the changes in its reflected spectra. The experiment is performed in a controlled humidity chamber, in which both temperature and humidity are measured and controlled by an ALTEC TH135 sensor. The RH and temperature resolutions are 1% and 0.1 ℃, with the corresponding dynamic ranges of 0% to 99% and −100 ℃ to 200 ℃, respectively. A double control and backup sensor (Novus Logbox RHT) is used with the RH resolution and dynamic range of 0.1% and 0% to 100% and the temperature resolution and dynamic range of 0.1 ℃ and −40 ℃ to 80 ℃. The temperature is maintained at 22 ℃, and the desired RH value is obtained by controlling the humidity flow rate. The prepared fiber tip is located within the chamber as shown in Fig. 6. The reflectance spectrum measuring setup is the same as that shown in Fig. 2.

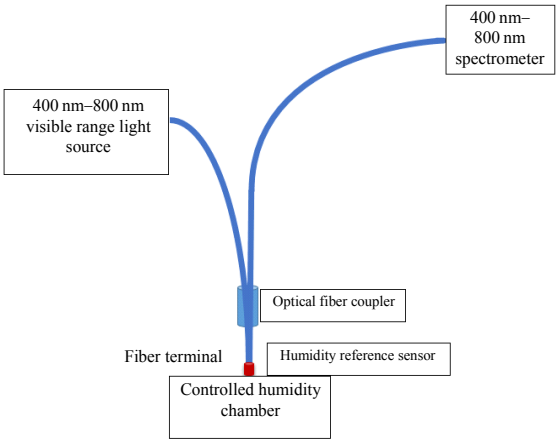

Fig. 6 Sensing setup for relative humidity measurement.

Humidity promotes the formation of the J-aggregate [30, 33], and the fiber is in the acidic (protonated) form. Therefore, the initial spectrum shows a peak at about 490 nm, attributed to the growth J-aggregate inducing resonant light scattering (RLS) at 490 nm [32] of approximately + 30% relative to the baseline. The RLS peak amplitude increases significantly because it is very narrow, with a bandwidth of about 12 nm; it reaches a maximum reflectance peak power almost 20% higher than the reference value presented in Fig. 3.

This peak indicates well-ordered J-aggregates; the functional film responds to RH by changing aggregate qualities; as noted previously, J-aggregate formation is favored by aqueous media [30, 32, 46].

The experimental setup allows sample exposure to a controlled environmental RH. Different RH levels are achieved within 1% precision. We study the reflectance spectrum around 490 nm under RH variations from 0% to 85%, at which the deposited J-aggregate film is stable on the fiber tip. The electrostatic binding of the TPPS J-aggregate to the fiber tip is low enough that the TPPS is washed away from the optical fiber tip under high RH. Therefore, the dynamic range of the proposed humidity sensor has a maximum limit of 85%, above which the coated thin film is destroyed. The reflectance spectra of the TPPS-coated film on the fiber end under different RH values are shown in Fig. 7.

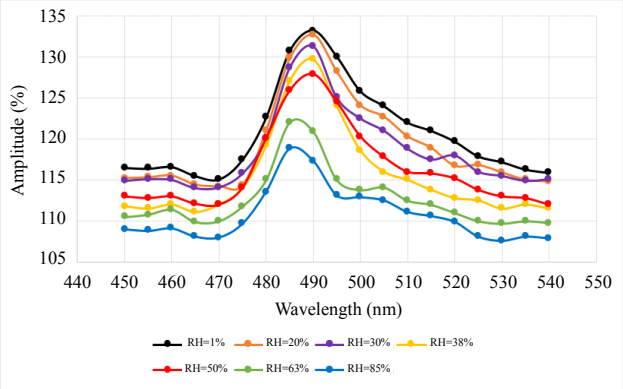

Fig. 7 Backscattered signals under different RH.

Both the refractive index and absorption coefficient depend on the environmental humidity. The coated thin film can be considered a low-quality factor random Fabry-Pérot (F-P) cavity structure [47]. The quasi-periodic variation of the reflected spectra in all curves of Fig. 7 arises from the low-quality-factor resonance frequency of the F-P structure.

No strict rule appears in the variation of spectral peak intensity with RH. As an example, the spectral peak intensities corresponding to 30%, 38%, and 50% RHs are equivalent, although the spectra are otherwise different. The peaks of the measured spectra depend on the number of experiments in each sequence, as well as the ages of given samples.

All experiments are performed at the room temperature and ambient pressure, and all experimental parameters except humidity are held constant. An RLS band from 488 nm to 493 nm is observed in Fig. 7. Because the vibrational and excitonic levels of the J-aggregate structure are decoupled, the measured results are expected to be independent of temperature and pressure; experimental verification of this expectation is under investigation and will be reported in the near future.

The variation of the RLS peak amplitude with RH is more sensitive to noise than the peak frequency shift, which is a characteristic of J-aggregates. Because of the weak electrostatic force between the TPPS J-aggregate and the fiber tip, for high RH, the TPPS molecules gradually separate from the fiber tip. In other words, aging occurs at high RH. To evaluate the effects of aging on the reflectance spectrum, a coated fiber is measured for several sequential weeks. The amplitude of the resonance peak shows a strong dependence on aging, but the redshift wavelength is independent of aging.

This effect is in agreement with the hysteresis result observed in our experiments. The resonance frequency does not change, but the amplitude decreases slowly after each experiment. The response time of wavelength change is about two minutes.

The resonance peak amplitude decreases over subsequent weeks. At high RH, aging appears sooner than that at low RH. The lifetime of the sensor is defined by the time average at which the RLS peak intensity reaches half of its initial value. In our experiments, the lifetime at high RH (>50%) is seven to ten days; at low RH (<25%), no variation in RLS peak intensity is observed. This indicates that the humidity sensor is very durable, such that aging is not a problem in sensor applications. However, the aging effect renders the amplitude of the resonance frequency peak unsuitable for humidity measurement; the redshift wavelength is more appropriate. Although aging does not affect the redshift frequency, it decreases the lifetime of the humidity sensor. This problem can be solved by using a suitable interface and protective layers in high-RH conditions. Nanoscale scratches on the optical fiber tip before deposition can improve the aging effect, for scratch dimensions of < 490 nm. This improvement arises from an increase in the electrostatic force between the TPPS film and fiber tip. These effects are under both theoretical and experimental investigations and will be reported in near future. Meanwhile, we expect to improve the film quality and stability by mixing TPPS with different polymers. In the next section, we will discuss wavelength shifts of the RLS peak.

4. Results

4.1 Chromatic response of coated fiber tip to humidity

The wavelengths of RLS for different RH levels are measured and are presented in Fig. 8. We prepare three different samples on the optical fiber tip. For each sample, we conduct measurements under 7 different RH levels. Measurements are conducted twice for each RH level. Thus, 42 measurements are conducted. The redshift of the RLS wavelength is decreased with increased RH. The average RLS wavelength varies by about 6 nm for RH variations between 0% and 85%. The accuracy of the RLS wavelength is 0.1 nm, which can be employed to determine the humidity sensor accuracy. The low errors in the RLS wavelength and the high RH dynamic range for this device indicate the suitability for various applications, such as intelligent agricultural engineering.

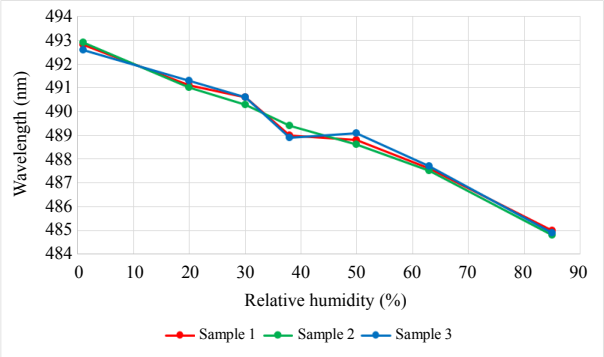

Fig. 8 RH level versus RLS peak wavelength.

4.2 Discussion and suggestion

This preliminary study outlines the responsiveness of TPPS thin films on optical fiber tips to humidity. The thin film can be removed over several cycles of exposure to high humidity. Aging decreases the intensity of the resonance frequency peak over several weeks, which requires further investigation. Other aspects for future study include improving the thickness control of the TPPS film, studying the response time, and improving the mobility of the fiber head by using different polymer coatings in the fiber cladding.

5. Conclusions

Our experimental analysis has shown that the amplitude is unsuitable for sensing the humidity, while sensors based on wavelength changes are viable. This is attributed to the water solubility of porphyrin and the promotion of J-aggregate formation by humidity. Different RH levels act as different microscale solvents; therefore, we expect different J-aggregate arrangements with different coupling coefficients. This is in agreement with the results reported previously [45, 46]. The measured wavelength of the RLS peak of the J-aggregate as a function of RH can be fitted by several polynomials. The best-fitting polynomial is of the fourth order. For low (< 25%) and high (> 50%) RHs, a linear approximation works well. The sensitivity $\partial\lambda_r / \partial RH$ is a function of RH, corresponding approximately to 1/12 nm / RH% for 1% RH.

References

[1] T. L. Yeo, T. Sun, and K. T. V. Grattan, "Fibre-optic sensor technologies for humidity and moisture measurement," *Sensors and Actuators A: Physical*, 2008, 144(2): 280–295.

[2] M. Giordano, M. Russo, A. Cusano, A. Cutolo, G. Mensitieri, and L. Nicolais, "Optical sensor based on ultrathin films of *δ*-form syndiotactic polystyrene for fast and high resolution detection of chloroform," *Applied Physics Letters*, 2004, 85(22): 5349–5351.

[3] A. Cusano, P. Pilla, L. Contessa, A. Iadicicco, S. Campopiano, A. Cutolo, *et al.*, "High-sensitivity optical chemosensor based on coated long-period gratings for sub-ppm chemical detection in water," *Applied Physics Letters*, 2005, 87(23): 234105-1–234105-3.

[4] S. Otsuki, K. Adachi, and T. Taguchi, "A novel fibre-optic gas sensing arrangement based on an air

gap setting and an application to optical detection of humidity," *Analytical Sciences*, 1998, 14(3): 633–635.
[5] S. J. Glenn, B. M. Cullum, R. B. Nair, D. A. Nivens, C. J. Murphy, and S. M. Angel, "Lifetime-based fiber-optic water sensor using a luminescent complex in a lithium-treated Nafion (TM) membrane," *Analytica Chimica Acta*, 2001, 448(1–2): 1–8.
[6] S. Q. Tao, C. B. Winstead, R. Jindal, and J. P. Singh, "Optical-fibre sensor using tailored porous sol-gel fiber core," *IEEE Sensors Journal*, 2004, 4(3): 322–328.
[7] M. Bedoya, M. T. Díez, M. C. M. Bondi, and G. Orellana, "Humidity sensing with a luminescent Ru (II) complex and phase-sensitive detection," *Sensors and Actuators B: Chemical*, 2006, 113(2): 573–581.
[8] S. Muto, O. Suzuki, T. Amano, and M. Morisawa, "A plastic optical fiber sensor for real-time humidity monitoring," *Measurement Science and Technology*, 2003, 14(6): 746–750.
[9] F. J. Arregui, Z. Ciaurriz, M. Oneca, and I. R. Matias, "An experimental study about hydrogels for the fabrication of optical fiber humidity sensors," *Sensors and Actuators B: Chemical*, 2003, 96(1–2): 165–172.
[10] A. Gastón, F. Pérez, and J. Sevilla, "Optical fiber relative-humidity sensor with polyvinyl alcohol film," *Applied Optics*, 2004, 43(21): 4127–4132.
[11] A. A. Herrero, H. Guerrero, and D. Levy, "High-sensitivity sensor of low relative humidity based on overlay on side-polished fibers," *IEEE Sensors Journal*, 2004, 4(1): 52–56.
[12] L. Xu, J. C. Fanguy, K. Soni, and S. Tao, "Optical fiber humidity sensor based on evanescent-wave scattering," *Optics Letters*, 2004, 29(11): 1191–1193.
[13] J. M. Corres, J. Bravo, I. R. Matias, and F. J. Arregui, "Nonadiabatic tapered single-mode fiber coated with humidity sensitive nanofilms," *IEEE Photonics Technology Letters*, 2006, 18(8): 935–937.
[14] P. Kronenberg, P. K. Rastogi, P. Giaccari, and H. G. Limberger, "Relative humidity sensor with optical fiber Bragg gratings," *Optics Letters*, 2002, 27(16): 1385–1387.
[15] S. Luo, Y. Liu, A. Sucheta, M. Evans, and R. V. Tassell, "Applications of LPG fiber optical sensors for relative humidity and chemical-warfare-agents monitoring," *Advanced Sensor Systems and Applications*, 2002, 4920: 193–205.
[16] K. M. Tan, C. M. Tay, S. C. Tjin, C. C. Chan, and H. Rahardjo, "High relative humidity measurements using gelatin coated long-period grating sensors," *Sensors and Actuators B: Chemical*, 2005, 110(2): 335–341.
[17] M. Konstantaki, S. Pissadakis, S. Pispas, N. Madamopoulos, and N. A. Vainos, "Optical fiber long-period grating humidity sensor with poly (ethylene oxide)/cobalt chloride coating," *Applied Optics*, 2006, 45(19): 4567–4571.
[18] S. H. Lim, L. Feng, J. W. Kemling, C. J. Musto, and K. S. Suslick, "An optoelectronic nose for detection of toxic gases," *Nature Chemistry*, 2009, 1(7): 562–567.
[19] K. M. Kadish, K. M. Smith, and R. Guilard, *Handbook of the Porphyrin: inorganic, organometallic and coordination chemistry*. Amsterdam, Netherlands: Elsevier, 2000.
[20] X. B. Zhang, Z. Z. Li, C. C. Guo, S. H. Chen, G. L. Shen, and R. Q. Yu, "Porphyrin-metalloporphyrin composite based optical fiber sensor for the determination of berberine," *Analytica Chimica Acta*, 2001, 439(1): 65–71.
[21] X. B. Zhang, C. C. Guo, Z. Z. Li, G. L. Shen, and R. Q. Yu, "An optical fiber chemical sensor for mercury ions based on a porphyrin dimer," *Analytical Chemistry*, 2002, 74(4): 821–825.
[22] R. Ni, R. B. Tong, C. C. Guo, G. L. Shen, and R. Q. Yu, "An anthracene/porphyrin dimer fluorescence energy transfer sensing system for picric acid," *Talanta*, 2004, 63(2): 251–257.
[23] G. Huyang, J. Canning, M. L. Aslund, D. Stocks, T. Khoury, and M. J, Crossley, "Evaluation of optical fiber microcell reactor for use in remote acid sensing," *Optics Letters*, 2010, 35(6): 817–819.
[24] R. Selyanchyn, S. Korposh, W. Yasukochi, and S. W. Lee, "A preliminary test for skin gas assessment using a porphyrin based evanescent wave optical fiber sensor," *Sensors & Transducers*, 2011, 125(2): 54–67.
[25] S. Stelitano, G. De Luca, S. Savasta, and S. Patané, "Polarized emission from high quality microcavity based on active organic layered domains," *Applied Physics Letters*, 2008, 93(19): 193302-1–193302-3.
[26] K. Araki, M. J. Wagner, and M. S. Wrighton, "Layer-by-layer growth of electrostatically assembled multilayer porphyrin films," *Langmuir*, 1996, 12(22): 5393–5398.
[27] Z. J. Zhang, S. F. Hou, Z. H. Zhu, and Z. F. Liu, "Preparation and characterization of a porphyrin self-assembled monolayer with a controlled orientation on gold," *Langmuir*, 2000, 16(2): 537–540.
[28] L. M. Scolaro, A. Romeo, M. A. Castriciano, G. De Luca, S. Patanè, and N. Micali, "Porphyrin deposition induced by UV irradiation," *Journal of the American Chemical Society*, 2003, 125(8): 2040–2041.
[29] G. D. Luca, G. Pollicino, A. Romeo, S. Patanè, and L. M. Scolaro, "Control over the optical and morphological properties of UV-deposited porphyrin structures," *Chemistry of Materials*, 2006, 18(23): 5429–5436.
[30] G. D. Luca, G. Pollicino, A. Romeo, and L. M. Scolaro, "Sensing behavior of tetrakis (4-sulfonatophenyl) porphyrin thin films," *Chemistry of Materials*, 2006, 18(8): 2005–2007.

[31] D. P. Bhopate, K. Kim, P. G. Mahajan, A. H. Gore, S. R. Patil, S. M. Majhi, *et al.*, "Fluorescent chemosensor for quantitation of multiple atmospheric gases," *Journal of Nanomed Nanotechnol*, 2017, 8(2): 1–9.

[32] A. Bahrampour, A. Iadicicco, G. D. Luca, M. Giordano, A. Borriello, A. Cutolo, *et al.*, "Porphyrin thin films on fibre optic probes through UV-light induced deposition," *Optics & Laser Technology*, 2013, 49: 279–283.

[33] A. Bahrampour, A. Iadicicco, G. D. Luca, M. Giordano, A. Cutolo, L. M. Scolaro, *et al.*, "Sensing characteristics to acid vapors of a TPPS coated fiber optic: a preliminary analysis," *World Academy of Science, Engineering and Technology*, *International Journal of Chemical, Molecular, Nuclear, Materials and Metallurgical Engineering*, 2012, 6(11): 989–992.

[34] G. De Luca, A. Romeo, V. Villari, N. Micali, I. Foltran, E. Foresti, *et al.*, "Self-organizing functional materials via ionic self assembly: porphyrins H- and J-aggregates on synthetic chrysotile nanotubes," *Journal of the American Chemical Society*, 2009, 131(20): 6920–6921.

[35] G. Scheibe, "Variability of the absorption spectra of some sensitizing dyes and its cause," *Angewandte Chemie*, 1936, 49: 563–564.

[36] G. Scheibe, "Über die veränderlichkeit der absorptionsspektren in lösungen und die nebenvalenzen als ihre ursache," *Angewandte Chemie*, 1937, 50(11): 212–219.

[37] E. E. Jelley, "Spectral absorption and fluorescence of dyes in the molecular state," *Nature*, 1936, 138(3502): 1009–1010.

[38] J. S. Briggs and A. Herzenberg, "Sum rules for the vibronic spectra of helical polymers," *Journal of Physics B: Atomic and Molecular Physics*, 1970, 3(12): 1663–1676.

[39] F. C. Spano and C. Silva, "H-and J-aggregate behavior in polymeric semiconductors," *Annual Review of Physical Chemistry*, 2014, 65: 477–500.

[40] M. Sauer and J. Hofkens, *Handbook of fluorescence spectroscopy and imaging: from ensemble to single molecules*. Hoboken, New Jersey, USA: John Wiley & Sons, 2010: 1–290.

[41] A. Eisfeld and J. S. Briggs, "The J- and H-bands of organic dye aggregates," *Chemical Physics*, 2006, 324(2–3): 376–384.

[42] R. H. Tredgold, "Langmuir-blodgett films: organic monolayer imaged," *Nature*, 1985: 313(6001): 348–348.

[43] K. M. Lenahan, Y. X. Wang, Y. Liu, R. O. Claus, J. R. Heflin, D. Marciu, *et al.*, "Novel polymer dyes for nonlinear optical applications using ionic self-assembled monolayer technology," *Advanced Materials*, 1998, 10(11): 853–855.

[44] A. Bahrampour, "New hollow core fiber design and porphyrin thin film deposition method towards enhanced optical fiber sensors," Ph.D. dissertation, University of Naples, Italy, 2013.

[45] R. F. Pasternack, P. R. Huber, P. Boyd, G. Engasser, L. Francesconi, E. Gibbs, *et al.*, "Aggregation of meso-substituted water-soluble porphyrins," *Journal of the American Chemical Society*, 1972, 94(13): 4511–4517.

[46] P. J. Collings, E. J. Gibbs, T. E. Starr, O. Vafek, C. Yee, L. A. Pomerance, *et al.*, "Resonance light scattering and its application in determining the size, shape, and aggregation number for supramolecular assemblies of chromophores," *The Journal of Physical Chemistry B*, 1999, 103(40): 8474–8481.

[47] A. G. Ardakani, S. M. Mahdavi, and A. R. Bahrampour, "Time-dependent theory for random lasers in the presence of an inhomogeneous broadened gain medium such as PbSe quantum dots," *Applied Optics*, 2013, 52(6): 1317–1324.